Journal of Biomechanics 47 (2014) 755–758

Contents lists available at ScienceDirect

Journal of Biomechanics

journal homepage: www.elsevier.com/locate/jbiomech
www.JBiomech.com

Short communication

Mechanical analysis of arterial plaques in native geometry with OCT wall motion analysis

Claire Robertson [a,b], Andrew E. Heidari [a,b,c], Zhongping Chen [a,b,c], Steven C. George [a,b,d,e,*]

[a] Department of Biomedical Engineering, University of California, Irvine, 2121 Engineering Hall, Irvine, CA 92617, USA
[b] The Edwards Lifesciences Center for Advanced Cardiovascular Technology, University of California, Irvine, USA
[c] Beckman Laser Institute, University of California, Irvine, CA 92617, USA
[d] Department of Chemical Engineering, University of California, Irvine, CA 92617, USA
[e] Department of Medicine, University of California, Irvine, CA 92617, USA

ARTICLE INFO

Article history:
Accepted 6 November 2013

Keywords:
Atherosclerotic plaque
Compliance
Optical coherence tomography

ABSTRACT

The mechanical behavior of an atherosclerotic plaque may encode information about the type, composition, and vulnerability to rupture. Human arterial segments with varying plaque burden were analyzed *ex vivo* with optical coherence tomography (OCT) to determine plaque type and to determine compliance during pulsatile inflation in their native geometry. Calcifications and lipid filled plaques showed markedly different compliance when analyzed with OCT wall motion analysis. There was also a trend towards increased circumferential variation in arterial compliance with increasing plaque burden.

1. Introduction

Atherosclerosis is the disease process that underpins the leading causes of morbidity and mortality in the western world can impact the entire arterial tree. The rupture of an atherosclerotic plaque is an acute event that can lead to sudden death. For example, in the coronary arteries, atherosclerotic plaque rupture is the most common trigger of myocardial infarction (Finn et al., 2010); plaque rupture in more peripherial arteries (e.g., carotid, femoral) can result in embolic stroke and death or permanent neurological deficit. Improved understanding of when and why arterial plaques fail or rupture could reduce the clinical burden of atherosclerosis (Roger et al., 2012).

Post mortem histological studies have established that certain classes of plaque are more likely to rupture (Cheruvu et al., 2007; Ma et al., 2006; Tang et al., 2009). For example, fibroatheromatous plaques comprised of a lipid pool covered by a thin fibrous cap tend to rupture and thrombose more frequently compared to fibrous overgrowths or calcified plaques (Cheruvu et al., 2007). However, clinical identification of these plaques remains challenging, as current clinically-used imaging techniques (e.g. intravascular ultrasound or angiography) lack the spatial resolution to identify key plaque features, such as the cap thickness (Schwartz and Touchard, 2010). Newer imaging techniques, including optical coherence tomography (OCT), have the requisite spatial resolution to definitively identify these plaques features (Jaffer, 2012; Suter et al., 2011); however, plaque structure by itself cannot fully define mechanical vulnerability. The ability to assess the mechanical behavior of a plaque *in situ* could further improve diagnosis and treatment of these lesions.

Current biomechanical methods are poorly adapted to assess the mechanical behavior of small, heterogeneous arterial plaques in their native milieu. *In vitro* biomechanical studies have established that arterial plaques have abnormal mechanical properties (Maher et al., 2009; Paini et al., 2007; Teng et al., 2009). The biomechanical properties of a plaque and its surrounding arterial tissue differ, and this difference may affect development and progression of a plaque (Schaar et al., 2006; Yang et al., 2008). Furthermore, vulnerable plaque types are filled with highly compliant lipid and thus, are more susceptible to deformation during the cardiac cycle (Schaar et al., 2006) compared to both the surrounding tissue or calcified plaques. However, traditional biomechanical methods require excision and extensive preparation, potentially affecting critical factors, such as arterial prestress (Cardamone et al., 2009; Horny et al., 2013). Furthermore, plaques may be mechanically heterogeneous: some evidence suggests that the border regions between the plaque and surrounding tissue are particularly vulnerable to rupture (Cheng et al., 1993; Schwartz et al., 2007). Finally, new methods with higher spatial resolution could determine whether these regions are more highly stressed or more compliant. A technique to simultaneously assess the mechanical behavior of an arterial plaque in their native geometry and its structural features could be useful to improve our understanding of plaque biomechanics, as well as to identify mechanically vulnerable plaques clinically.

* Corresponding author at: University of California, Department of Biomedical Engineering, 2420 Engineering Hall, Irvine, CA 92697-2730, United States.
Tel.: +1 949 824 3941; fax: +1 949 824 9968.
E-mail address: scgeorge@uci.edu (S.C. George).

0021-9290/$ - see front matter © 2013 Elsevier Ltd. All rights reserved.
http://dx.doi.org/10.1016/j.jbiomech.2013.11.010

Our group has developed high resolution techniques to simultaneously assess tissue structure and biomechanical properties based on endoscopic OCT (Qi et al., 2012; Robertson et al., 2011). Unlike previous methods to assess tissue biomechanics with OCT, this method is clinically translatable. The high resolution technique analyzes tissue in its native configuration using cyclic loading and has been previously validated against elastic phantoms of similar size and geometry (Robertson et al., 2011). The current study sought to establish whether wall motion analysis from OCT was feasible in an *in vitro* physiological arterial preparation, and to analyze the mechanical behavior of plaques in their native geometry. We hypothesized that arterial plaques would differ mechanically from the surrounding tissue, and that mechanical behavior would depend on plaque type.

2. Materials and methods

2.1. Experimental setup

Imaging studies were performed on human cadaveric arterial samples from the common femoral artery. 10 cm long regions were harvested at autopsy from ten donors of varying age and health (Table 1), wrapped in saline soaked gauze and frozen at −20 °C until imaging. While freezing can affect arterial compliance (Venkatasubramanian et al., 2010), all specimens were handled similarly. On the day of imaging, the vessels were cannulated, side branches were sealed with suture and specimens were immersed in saline. Using a peristaltic pump and a 5PSI pressure transducer, 1 Hz, pulsatile flow (0–10 mmHg) of saline through the vessel was established. Vessels were then allowed to acclimate to perfusion for at least 5 min.

2.2. Imaging

During pulsatile (1 Hz) inflation, the vessels were imaged with OCT. Using two-way valves, an endoscopic OCT probe was introduced to the lumen of the artery. The OCT system used has been described previously (Lee et al., 2011). Briefly, light from a swept source laser (CW 1310 nm, FWHM 100 nm, power 5 mW, scan rate 20 kHz) was passed through a fiber based Michelson Interferometer consisting of a 90:10 1 × 2 inline fiber coupler, two inline fiber circulators, an in air variable optical delay reference arm, and a 50:50 2 × 2 fiber coupler connected to a balanced photodetector. The sample arm of the interferometer was connected to a helical scanning MEMS endoscopic probe to image the sample lumen at 20 Hz. The maximum axial scan range of this system was determined experimentally to be 2.9 mm, with axial and lateral resolutions (in saline) of 6 μm and 15 μm, respectively.

Images of the same axial location were acquired during 10 s of pulsatile flow. These images were then analyzed as previously described to extract wall motion and relative compliance (Robertson et al., 2011). Briefly, the tissue surface was identified in each serial image, motion at the driving frequency over several cardiac cycles was isolated using Fourier domain filtering, and pressure was compared to deformation at each of 1200 radial locations, resulting in a measure of surface deformation termed wall compliance. Wall compliance is related to both integrated elastic modulus for the subsurface tissue and tissue thickness. Previous work has demonstrated high reliability of these methods (Robertson et al., 2011). Locations where artifacts obscured the tissue surface were rejected. For each arterial specimen, 3–7 axial locations were imaged and analyzed.

Plaques visible on these axial OCT images were identified and classified using previously described criteria (Yabushita et al., 2002). Signal-poor plaques with a thin cap and diffuse border were classified as fibroatheroma, signal-poor plaques with sharp borders were classified as calcified, and signal rich plaques were classified as fibrous overgrowths (Fig. 1).

Table 1
Donor demographics

Age	Gender	Cause of death	Plaque number	Compliance $(Pa^* mm)^{-1}$
20	M	Melanoma	0	5+3.4E−8
67	F	Cirrhosis of the liver	5	4.6+1.8E−8
80	F	Metastatic neuroendocrine cancer	1	4.5+1.4E−8
89	F	Stroke and aspiration pneumonia	6	8.8+3E−8
91	F	Alzheimers disease and cardiac arrest	8	9+4.3E−7
95	M	Bladder carcinoma and cardiac arrest	11	2.3+1.8E−8

2.3. Statistical analyses

Mean arterial compliance and variance in arterial compliance were compared across donors using ANOVA and Levine's test for unequal variance to determine variability with donor. Variability in arterial compliance was also regressed with number of arterial plaques to determine if decreased arterial health affected the variability in arterial compliance. Plaque type and mechanical behavior were also analyzed: for each class of plaque analyzed, (fibroatheroma, calcification), mean compliance over the surface of the plaque was compared to mean compliance at the same axial location. Sensitivity and specificity of altered plaque compliance for plaque classification was then calculated.

3. Results

Donor demographic information, number of plaques in the entire arterial segment, and average arterial compliance are summarized in Table 1. Thirty-one arterial lesions were identified on OCT images, of which eight were identified as fibroatheroma, eight as calcifications, four as fibrous overgrowths and nine were unclear due to insufficient image quality (Fig. 1). Higher numbers of plaques were generally seen in specimens from older donors, and donors with a history of cardiovascular disease (not analyzed statistically). No difference in mean arterial compliance was seen with increasing number of plaques ($R^2 < 0.1$). Arterial regions with high plaque burdens were noted to have increased variability in compliance (Fig. 2). Levine's test for uneven variance confirmed different variations in arterial compliance between donors. Standard deviation of compliance was then regressed with plaque number, showing a trend suggesting increased variability in compliance with increased number of plaques ($R^2=0.45$, $p=0.08$- Fig. 3).

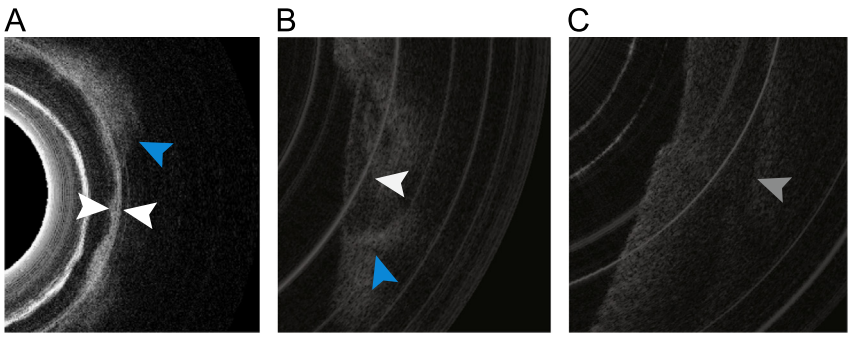

Fig. 1. OCT images of different arterial formations. (A) Lipid filled plaque – Note the thin cap (white arrows), diffuse border (blue arrow) and dark, signal poor body. (B) Calcified plaque – Sharp borders (blue arrow) and mottled, signal bright plaque body (white arrow). (C) Healthy arterial wall. Note the boundary between intima and media (gray arrow). (For interpretation of the references to color in this figure legend, the reader is referred to the web version of this article.)

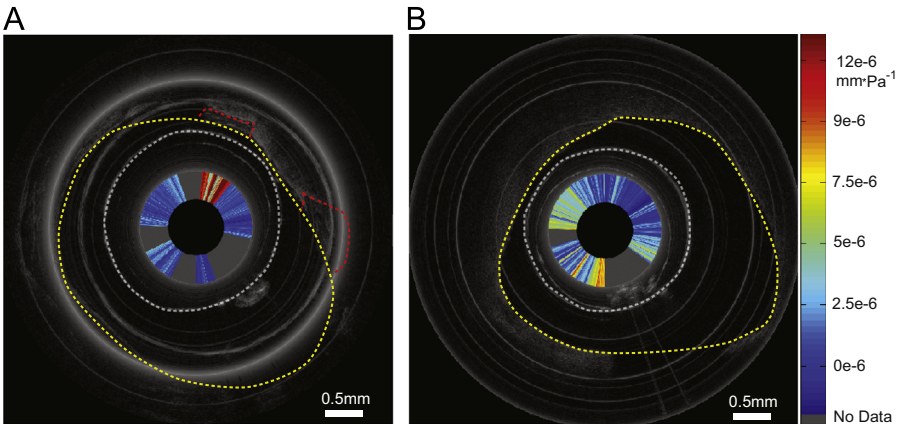

Fig. 2. OCT images and wall motion compliance analysis for two sample arterial segments. The surface of the OCT probe is outlined in white, the surface of the arterial specimen is outlined in yellow, and plaques are outlined in red. Panel A includes a number of arterial plaques. The compliance in this region was 4.2 ± 3.8 (Pa mm)$^{-1}$. Panel B shows a healthy region with a strong border between intima and media. The compliance in this region was 4.5 ± 2.5 (Pa mm)$^{-1}$. Note the 50% higher standard deviation in panel A. (For interpretation of the references to color in this figure legend, the reader is referred to the web version of this article.)

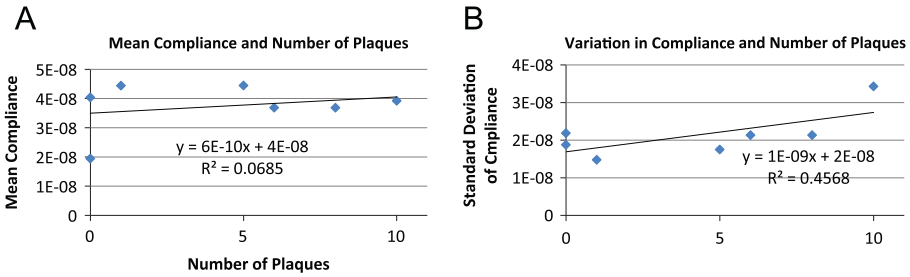

Fig. 3. Relationship between arterial plaque burden and compliance. (A) The regression of plaque number with mean compliance, showing little correlation between increasing plaque number and mean arterial compliance. (B) The regression of plaque number with variation in arterial compliance, showing increased variability with higher plaque burden.

Compliance was then compared between vulnerable and calcified plaques (Fig. 4). Too few fibrous plaques were identified for statistical analysis. Lipid-filled plaques (fibroatheromas) were significantly softer (compliance was $117+20\%$ of the surrounding tissue, $p<0.01$) than the surrounding tissue whereas calcified plaques were noted to be stiffer (compliance was $81+16\%$ of the surrounding tissue, $p<0.01$). The sensitivity and specificity of plaque compliance for distinguishing plaque type were 0.88 and 0.77, respectively.

4. Discussion

OCT offers promise for diagnosis and classification of arterial plaques. In this study, we demonstrated the feasibility of OCT wall motion analysis to assess the mechanical properties of arteries during cyclic loading similar to that seen *in vivo*. While several previous works have suggested methods to analyze arterial plaque biomechanics with OCT, this is the first work to use the native arterial geometry and physiologic inflation. The methods used mimicked important challenges of *in vivo* arterial imaging, including dynamic pulsatile inflation and concomitant probe motion, which limit image quality. Additionally, this study simultaneously identified plaque type and compliance. Morphology on OCT imaging has been previously established as a reliable diagnostic of plaque type (Yabushita et al., 2002), and was thus used in this study. OCT wall motion analysis has been used previously *in vivo*, and thus has high potential for clinical translation.

While no correlation was noted between plaque number and mean compliance samples with higher plaque burdens tended to display higher variability in compliance. As atherosclerosis is traditionally described as a "hardening of the arteries," the finding that the more affected specimens did not differ in mean compliance was somewhat surprising. Higher variability, on the other hand, is consistent with the finding that plaques are mechanically different from their embedding tissue. Compliance and plaque type were shown to be associated in the current study, which is consistent with previous studies that used IVUS palpography (Brugaletta et al., 2012; Schaar et al., 2003, 2004, 2006) and *in vitro* biomechanical testing. The vulnerability of a plaque depends on several features, such as its size and load patterns, which have been linked to histological parameters including size, cap thickness, and remodeling index (Ohayon et al., 2008). The ability to assess the deformations in the plaque in a physiological setting is a major strength of this study. While the technique described focuses on strain in the radial direction, strain in the orthogonal direction may be identifiable with this form of imaging. Mechanical compliance may also serve as a plaque classifier: in this study compliance and plaque type were strongly associated. When morphology alone is insufficient to categorize a plaque, its deformations under loading may offer additional diagnostic information.

The limitations of this study are related to the *ex vivo* experimental setup. Human cadaveric tissue and pulsatile inflation were used to mimic the challenging *in vivo* imaging scenario. However, the samples were sourced from the femoral artery and had undergone one freeze–thaw cycle before testing. The femoral artery may be mechanically different from the coronary arteries, or other clinically important sites of atherosclerosis, and display a different frequency of plaque type. However, the methods used in this work are translatable to the assessment of plaque in multiple clinically important locations. Furthermore, previous work suggests that femoral arterial plaques are not mechanically or structurally different from coronary or carotid arterial plaques (de Korte et al., 2000). In order to image in one session, samples were frozen,

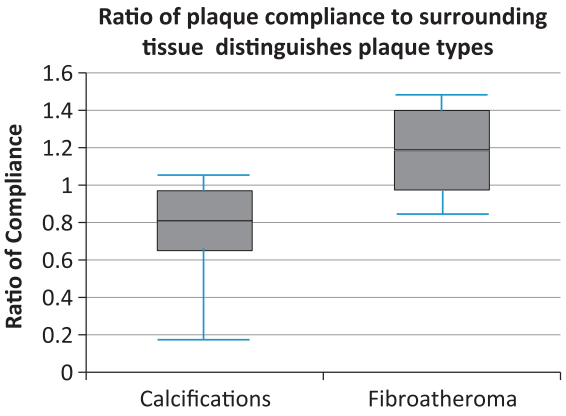

Fig. 4. Plaque compliance compared to compliance of the surrounding arterial tissue. Lipid filled plaques are relatively soft and calcified plaques are relatively stiff compared to the surrounding tissue.

though freeze–thaw cycles are known to change the mechanical behavior of arterial tissue (Venkatasubramanian et al., 2010). The inflation pressures used in this study were lower than pressures seen *in vivo*. Even so, differences in plaque biomechanics were observed, suggesting that even greater deformations and differences in strain patterns could be present *in vivo*. Similarly, the adventitial tissue surrounding the artery was not present, which may affect the material behavior of the artery, but should have minimal impact on the mechanical property of the plaque, and should affect the entire artery homogeneously.

In summary, mechanical behavior of atherosclerotic plaques may offer additional diagnostic information. In an *ex vivo* preparation that mimicked key *in vivo* features including cyclic loading, we demonstrated using OCT wall motion analysis that plaque compliance and type were associated, and that arterial segments with increased plaque burden showed higher variability in compliance. Thus, OCT may be useful in the clinical assessment of arterial plaques *in vivo*.

Conflict of interest statement

Zhongping Chen is a partial owner of OCT Medical. There are no other conflicts of interest to report.

Acknowledgments

We would like to acknowledge UCI anatomical services and persons who donate their bodies to science. Thanks to Joe Jing for help with experimental setup. Funding: NSF GRFP, ARCS Inc, NIH R01HL067954 and R01EB010090.

References

Brugaletta, S., Garcia-Garcia, H.M., Serruys, P.W., Maehara, A., Farooq, V., Mintz, G.S., de Bruyne, B., Marso, S.P., Verheye, S., Dudek, D., Hamm, C.W., Farhat, N., Schiele, F., McPherson, J., Lerman, A., Moreno, P.R., Wennerblom, B., Fahy, M., Templin, B., Morel, M.A., van Es, G.A., Stone, G.W., 2012. Relationship between palpography and virtual histology in patients with acute coronary syndromes. JACC Cardiovascular Imaging 5 (3 Suppl), S19–27.

Cardamone, L., Valentin, A., Eberth, J.F., Humphrey, J.D., 2009. Origin of axial prestretch and residual stress in arteries. Biomech. Modeling Mechanobiol. 8, 431–446.

Cheng, G.C., Loree, H.M., Kamm, R.D., Fishbein, M.C., Lee, R.T., 1993. Distribution of circumferential stress in ruptured and stable atherosclerotic lesions. A structural analysis with histopathological correlation. Circulation 87, 1179–1187.

Cheruvu, P.K., Finn, A.V., Gardner, C., Caplan, J., Goldstein, J., Stone, G.W., Virmani, R., Muller, J.E., 2007. Frequency and distribution of thin-cap fibroatheroma and ruptured plaques in human coronary arteries: a pathologic study. J. Am. Coll. Cardiol 50, 940–949.

de Korte, C.L., Pasterkamp, G., van der Steen, A.F.W., Woutman, H.A., Bom, N., 2000. Characterization of plaque components with intravascular ultrasound elastography in human femoral and coronary arteries in vitro. Circulation 102, 617–623.

Finn, A.V., Nakano, M., Narula, J., Kolodgie, F.D., Virmani, R., 2010. Concept of vulnerable/unstable plaque. Arterioscler. Thromb. Vasc. Biol. 30, 1282–1292.

Horny L., Adamek T., Kulvajtova M. Analysis of axial prestretch in the abdominal aorta with reference to post mortem interval and degree of atherosclerosis. J. Mech. Behav. Biomed. Mater. http://dx.doi.org/10.1016/j.jmbbm.2013.01.033, in press.

Jaffer, F.A., 2012. Shining light and illuminating murine atherosclerosis via optical coherence tomography. Arterioscler. Thromb. Vasc. Biol. 32, 1068–1069.

Lee, S.W., Heidary, A.E., Yoon, D., Mukai, D., Ramalingam, T., Mahon, S., Yin, J., Jing, J., Liu, G., Chen, Z., Brenner, M., 2011. Quantification of airway thickness changes in smoke-inhalation injury using in-vivo 3-D endoscopic frequency-domain optical coherence tomography. Biomed. Opt. Express 2, 243–254.

Ma, H., Aziz, K.S., Huang, R., Abela, G.S., 2006. Arterial wall cholesterol content is a predictor of development and severity of arterial thrombosis. J. Thromb. Thrombolysis 22, 5–11.

Maher, E., Creane, A., Sultan, S., Hynes, N., Lally, C., Kelly, D.J., 2009. Tensile and compressive properties of fresh human carotid atherosclerotic plaques. J. Biomech. 42, 2760–2767.

Ohayon, J., Finet, G., Gharib, A.M., Herzka, D.A., Tracqui, P., Heroux, J., Rioufol, G., Kotys, M.S., Elagha, A., Pettigrew, R.I., 2008. Necrotic core thickness and positive arterial remodeling index: emergent biomechanical factors for evaluating the risk of plaque rupture. Am. J. Physiol. Heart Circ. Physiol. 295, H717–727.

Paini, A., Boutouyrie, P., Calvet, D., Zidi, M., Agabiti-Rosei, E., Laurent, S., 2007. Multiaxial mechanical characteristics of carotid plaque: analysis by multiarray echotracking system. Stroke 38, 117–123.

Qi, W., Chen, R., Chou, L., Liu, G., Zhang, J., Zhou, Q., Chen, Z., 2012. Phase-resolved acoustic radiation force optical coherence elastography. J. Biomed. Opt. 17, 110505.

Robertson, C., Lee, S.W., Ahn, Y.C., Mahon, S., Chen, Z., Brenner, M., George, S.C., 2011. Investigating in vivo airway wall mechanics during tidal breathing with optical coherence tomography. J. Biomed. Opt. 16, 106011.

Roger, V.L., Go, A.S., Lloyd-Jones, D.M., Benjamin, E.J., Berry, J.D., Borden, W.B., Bravata, D.M., Dai, S., Ford, E.S., Fox, C.S., Fullerton, H.J., Gillespie, C., Hailpern, S. M., Heit, J.A., Howard, V.J., Kissela, B.M., Kittner, S.J., Lackland, D.T., Lichtman, J. H., Lisabeth, L.D., Makuc, D.M., Marcus, G.M., Marelli, A., Matchar, D.B., Moy, C. S., Mozaffarian, D., Mussolino, M.E., Nichol, G., Paynter, N.P., Soliman, E.Z., Sorlie, P.D., Sotoodehnia, N., Turan, T.N., Virani, S.S., Wong, N.D., Woo, D., Turner, M.B., 2012. Heart disease and stroke statistics—2012 update: a report from the American Heart Association. Circulation 125, e2–e220.

Schaar, J.A., de Korte, C.L., Mastik, F., Baldewsing, R., Regar, E., de Feyter, P., Slager, C. J., van der Steen, A.F., Serruys, P.W., 2003. Intravascular palpography for high-risk vulnerable plaque assessment. Herz 28, 488–495.

Schaar, J.A., Regar, E., Mastik, F., McFadden, E.P., Saia, F., Disco, C., de Korte, C.L., de Feyter, P.J., van der Steen, A.F., Serruys, P.W., 2004. Incidence of high-strain patterns in human coronary arteries: assessment with three-dimensional intravascular palpography and correlation with clinical presentation. Circulation 109, 2716–2719.

Schaar, J.A., van der Steen, A.F., Mastik, F., Baldewsing, R.A., Serruys, P.W., 2006. Intravascular palpography for vulnerable plaque assessment. J. Am. Coll. Cardiol. 47, C86–91.

Schwartz, R., Touchard, A., 2010. Detecting vulnerable plaque using invasive methods. In: Naghavi, M. (Ed.), Asymptomatic Atherosclerosis. Humana Press, New York, pp. 475–481.

Schwartz, S.M., Galis, Z.S., Rosenfeld, M.E., Falk, E., 2007. Plaque rupture in humans and mice. Arterioscler. Thromb. Vasc. Biol. 27, 705–713.

Suter, M.J., Nadkarni, S.K., Weisz, G., Tanaka, A., Jaffer, F.A., Bouma, B.E., Tearney, G.J., 2011. Intravascular optical imaging technology for investigating the coronary artery. JACC Cardiovasc. Imaging 4, 1022–1039.

Tang, D., Teng, Z., Canton, G., Yang, C., Ferguson, M., Huang, X., Zheng, J., Woodard, P. K., Yuan, C., 2009. Sites of rupture in human atherosclerotic carotid plaques are associated with high structural stresses: an in vivo MRI-based 3D fluid–structure interaction study. Stroke 40, 3258–3263.

Teng, Z., Tang, D., Zheng, J., Woodard, P.K., Hoffman, A.H., 2009. An experimental study on the ultimate strength of the adventitia and media of human atherosclerotic carotid arteries in circumferential and axial directions. J. Biomech. 42, 2535–2539.

Venkatasubramanian, R.T., Wolkers, W.F., Shenoi, M.M., Barocas, V.H., Lafontaine, D., Soule, C.L., Iaizzo, P.A., Bischof, J.C., 2010. Freeze–thaw induced biomechanical changes in arteries: role of collagen matrix and smooth muscle cells. Ann. Biomed. Eng. 38, 694–706.

Yabushita, H., Bouma, B.E., Houser, S.L., Aretz, H.T., Jang, I.K., Schlendorf, K.H., Kauffman, C.R., Shishkov, M., Kang, D.H., Halpern, E.F., Tearney, G.J., 2002. Characterization of human atherosclerosis by optical coherence tomography. Circulation 106, 1640–1645.

Yang, C., Tang, D., Kobayashi, S., Zheng, J., Woodard, P.K., Teng, Z., Bach, R., Ku, D.N., 2008. Cyclic bending contributes to high stress in a human coronary atherosclerotic plaque and rupture risk: in vitro experimental modeling and ex vivo MRI-based computational modeling approach. Mol. Cell. Biomech. 5, 259–274.